

Tumor growth instability and the onset of invasion

Mario Castro,¹ Carmen Molina-París,² and Thomas S. Deisboeck³

¹*Grupo Interdisciplinar de Sistemas Complejos (GISC) and Grupo de Dinámica No Lineal (DNL),*

Escuela Técnica Superior de Ingeniería (ICAI), Universidad Pontificia Comillas, E-28015 Madrid, Spain

²*Department of Applied Mathematics, University of Leeds, Leeds LS2 9JT, United Kingdom and Departamento de Matemáticas,*

Física Aplicada y Físico-química, Facultad de Farmacia, Universidad San Pablo CEU, E-28660 Madrid, Spain

³*Complex Biosystems Modeling Laboratory, Harvard-MIT (HST) Athinoula A. Martinos Center for Biomedical Imaging,*

Massachusetts General Hospital, Charlestown, Massachusetts 02129, USA

(Received 15 March 2005; published 6 October 2005)

Motivated by experimental observations, we develop a mathematical model of chemotactically directed tumor growth. We present an analytical study of the model as well as a numerical one. The mathematical analysis shows that: (i) tumor cell proliferation by itself cannot generate the invasive branching behavior observed experimentally, (ii) heterotype chemotaxis provides an instability mechanism that leads to the onset of tumor invasion, and (iii) homotype chemotaxis does not provide such an instability mechanism but enhances the mean speed of the tumor surface. The numerical results not only support the assumptions needed to perform the mathematical analysis but they also provide evidence of (i), (ii), and (iii). Finally, both the analytical study and the numerical work agree with the experimental phenomena.

DOI: [10.1103/PhysRevE.72.041907](https://doi.org/10.1103/PhysRevE.72.041907)

PACS number(s): 87.18.Hf, 87.18.Ed, 87.17.Aa, 82.39.Rt

I. INTRODUCTION

Experiments have shown that a variety of tumor cells produce both protein growth factors and their corresponding receptors, enabling a mechanism termed *autocrine* or *paracrine*, if the stimulus not only affects the *source* but also its bystander cells [1]. Such polypeptide growth factors can, for example, stimulate tumor cell growth and invasion, such as in the case of hepatocyte growth factors [2] and epidermal growth factor [3], or induce tumor angiogenesis through secretion of vascular endothelial growth factor [4] (VEGF). The biological evidence supporting these paracrine/autocrine loops suggests that such signaling factors have significance for cell-cell interaction [5]. Depending on the cancer type, its characteristic features include a combination of rapid volumetric growth and genetic/epigenetic heterogeneity, as well as extensive tissue invasion with both local and distant dissemination. Such tumor cell motility has been intensely investigated and found to be guided by diffusive chemical gradients, a process called chemotaxis, e.g., Ref. [6]. Since cell signaling and information processing on the microscopic scale should also determine the emergence of both multicellular patterns and macroscopic disease dynamics, it is intriguing to characterize the relationship between environmental stimuli and the cell-signaling *code* they trigger.

In a recent paper, Sander and Deisboeck [7] showed that a combined heterotype and homotype diffusive chemical signal can yield invasive cell branching patterns seen in microscopic brain tumor experiments [8] by means of a discrete model, for some specific form of the interactions. There is a long history on the study of this type of assay [4,9]. There are also quite a few mathematical models that address the issue of tumor growth and cell migration [10–19] as well as two review papers [20,21] that focus on the state of the art of macroscopic modeling of solid tumours and on multicellular systems and the derivation of macroscopic equations from a microscopic description, respectively. Reference [22] is a

phenomenological approach to model prevascular tumor growth. In Ref. [7] the authors carry out a linear stability analysis from the steady state and show that both homotype and heterotype chemotaxis are required for the development of invasive branching behavior. Employing an improved version of our previously developed reaction-diffusion model [23], we now specifically investigate the relationship between an extrinsic nutrient signal, heterotype chemoattractant Q , and the homotype soluble signal C , produced by the tumor cells themselves. The underlying oncology concept is that in the process of spatiotemporal tumor expansion, C functions as a guiding *cue* for mobile cancer cells, directing the trailing ones towards sites of higher Q concentration and thus avoiding tissue areas with low or decreasing density of Q . In a sense, the dynamically changing C profile, secreted by the tumor cells, encodes the underlying Q map, which in itself represents a particular tissue environment. However, this picture is difficult to quantitatively assess with conventional experimental assays, and it has not yet been theoretically demonstrated in a clear-cut way.

In this paper, we are therefore particularly interested in how these mechanisms, homotype and heterotype chemotaxis, compete and/or cooperate in the formation of tumor branching structures and how the mathematical reaction terms must be chosen in order to reproduce, with some degree of universality, the experimentally observed patterns. Thus, we will study the impact of a fixed extrinsic nutrient source, and how the interplay among nutritive, mechanical and chemical properties support the principle of *least resistance, most attraction* for spatio-temporal tumor cell expansion [8]. The analytical and numerical results provide insight as to the cells' ability to readily modulate C , as well as, more generally, to the importance of paracrine growth factors for information transfer in multicellular biosystems. We have kept the mathematical model as general as possible in order to understand the essential features of the time evolution of the system.

The report of our results is organized as follows. We describe our reaction-diffusion mathematical model in Sec. II, where a detailed discussion of each of the involved mechanisms is given separately. Section III reports general analytical results for the model of Sec. II. We numerically check the validity of our analytical results in Sec. IV. Finally, we conclude in Sec. V with a discussion of our results and provide a picture of chemotactic cell invasion as triggered by tumor growth instability.

II. MATHEMATICAL MODEL

Tumor expansion is a multistep process that involves, in a nontrivial fashion, several mechanisms of progression. Here, we concentrate on tumor cell proliferation and chemotactically guided invasion, induced by both a diffusive heterotype and a homotype attractant (produced by the very tumor cells).

A. Extracellular matrix gel (matrigel)

The experimental setting, which we have modeled here, consisted of a multicellular tumor spheroid (MTS) embedded in a tissue culture medium-enriched extracellular matrix (ECM) gel, Matrigel [8]. We consider $M=M(\mathbf{x}, t)$, the average density field of the gel matrix as a function of space \mathbf{x} and time t . The role of M is twofold. From a nutrient perspective, the tumor cells [whose concentration will be described by the density field $U(\mathbf{x}, t)$ hereafter] metabolize M and, hence, they are able to proliferate. Besides, from a mechanical perspective, the solid gel matrix has an impact on tumor cell mobility, i.e., it confines the tumor cells and so they are guided by *least or lesser resistance* areas throughout the ECM here *in vitro*, or, *in vivo*, by the distinct mechanical properties of the surrounding tissue. Therefore, at a particular site, more M can sustain a higher concentration of tumor cells, which in turn will metabolize more of the nourishing gel medium and thus, over time, will lead to an on-site reduction of the ECM matrix' mechanical resistance, which had initially hindered cell motility.

Mathematically, we assume that the consumption rate of M by U , which we denote by $R_M(M, U)$, grows monotonically with both variables, and is a non-negative function. Later, we will make some assumptions regarding the mechanical impact of M on the diffusivity of tumor cells and of both heterotype and homotype chemoattractants.

For the sake of generality, we assume that the matrigel medium can diffuse, with constant diffusivity μ_M . The order of magnitude of μ_M depends on the specific type of medium under consideration (see Sec. III A for further discussion on this issue). In summary, we can write the following equation for the matrigel M

$$\partial_t M = \mu_M \nabla^2 M - \lambda_M R_M(M, U), \quad (1)$$

where λ_M is the inverse of the characteristic time of the M consumption process. Equation (1) reflects the fact that the matrigel nutrient is metabolized by the tumor cells and not replenished.

B. Heterotype chemoattractant

Chemotaxis can be generally defined as motility induced and guided by a concentration gradient. As in our previous model [23], the heterotype chemoattractant represents nutrients diffusing from a source, e.g., *in vivo*, a blood vessel, and as such is what should guide both on-site cell proliferation and the onset of invasion. Chemotaxis has been extensively studied in the literature [24,25]. It is generically assumed that the chemotactic flux takes the form

$$\mathbf{J}_{chem} = \chi_Q(Q, M) U \nabla Q.$$

Note that this flux is proportional to the tumor cell concentration U . The function $\chi_Q(Q, M)$ is usually called the chemotactic sensitivity, and is a positive decreasing (or at least constant) function of both arguments Q and M . The explicit dependence of χ_Q on M reflects the effect of the mechanical *pressure* of the underlying medium, that constrains both tumor cell and heterotype chemoattractant movement. Besides, tumor cells digest chemoattractant molecules, so as the former move towards a positive gradient of Q , the concentration of Q diminishes. This reduction is governed by the reaction term $R_Q(Q, U)$.

Combining these ideas, we obtain the following equation for the heterotype chemoattractant field density Q :

$$\partial_t Q = \nabla[\mu_Q(M) \nabla Q] - a_Q R_Q(Q, U), \quad (2)$$

where a_Q is the inverse of the characteristic time of the Q consumption process.

In the experimental *in vitro* setting modeled here, the heterotype chemoattractant was supplied externally. Acknowledging that the original experimental setting [8] used a non-replenished nutrient source, here, for simplicity, we model a replenished source of Q and Eq. (2) thus has to be supplemented accordingly. This can be modeled by means of the following boundary condition:

$$Q(x=L, t) = Q_0, \quad (3)$$

for one-dimensional systems, where L is the size of the system, and

$$Q(x=L_x, y, t) = Q_0, \quad (4)$$

for two-dimensional ones, where L_x is the horizontal size of the system and L_y the vertical one.

C. Homotype chemoattractant

Tumor cells have been shown to produce protein growth factors such as the transforming growth factor alpha (TGF- α). These growth factors can affect the tumor producing cell itself, hence, generate an "autocrine" feedback loop, as well as bystander cells, an effect called "paracrine" [26]. In the following, we refer to this soluble chemical effector, as homotype chemoattractant and we denote by C its density field.

Since an ever growing population of tumor cells digests more Q , the homotype chemoattractant C may take over at some point as *guidance cue* in the regions with low Q concentration. First, we assume that the homotype chemoattractant is both released and internalized, or (for the purposes

here), taken up or consumed by the tumor cells. The latter is based on a ligand-receptor interaction and thus on internalization of the class of protein growth factors, which C represents. Note, that if all cells produce C , a cell close to the main tumor would be less *inclined* to move away from it, since it is close to a large basin of C . One could tune the production rate of C in such a way as to ensure that only the density profile of C near the tumor surface has an impact on the “decision” of a tumor cell to stay (proliferate) or to start moving (invasion). This effect should have an impact on the tumor cell density U .

The above discussion implies that C is also chemotactic for U . The main difference with the heterotype chemoattractant Q is that the homotype chemoattractant C is produced (and consumed) by the tumor cells. We denote by $R_C^{(p)}(M, U)$ and $R_C^{(d)}(C, U)$ the production and digestion rates of C , respectively. Earlier studies have shown [27–29] that eventually a central dead area develops due to the lack of nutrients inside the tumor spheroid, which in turn leads to the release of growth inhibitory factors from the dying cells [30]. A full consideration of the development of such a *necrotic core* is out of the scope of this paper [31]. We consider the existence of this “dead area” in the dependence of R_C^p on the matrigel density M . This dependence means that the production of C is enhanced where M is high (outside the main tumor, as inside the tumor the matrigel has been degraded) and therefore, the production of C is maximized for *reactive* tumor cells, i.e., surface tumor cells outside the necrotic core of the tumor [8]. We also assume that $\chi_Q(Q, M)$ is typically larger than the chemotactic sensitivity of C , $\chi_C(C, M)$, for the concentrations involved in the problem and that $\chi_C(C, M)$ depends both on C and M . The explicit dependence of χ_C on M reflects the fact that the matrigel constrains homotype chemoattractant movement as well. Finally, C also diffuses with diffusion coefficient $\mu_C(M)$.

In summary, the homotype chemoattractant obeys the following equation:

$$\partial_t C = \nabla[\mu_C(M) \nabla C] + \alpha_C R_C^{(p)}(M, U) - a_C R_C^{(d)}(C, U), \quad (5)$$

where α_C and a_C are the inverse of the characteristic time of the C production and consumption process, respectively.

D. Tumor cells

The *global nutrient* density available to tumor cells is proportional to the medium density M . We then assume that tumor cells proliferate with a rate that is proportional to the rate of consumption of M . Moreover, we consider that tumor cells diffuse with a diffusion coefficient μ_U , and that μ_U depends on M to reflect the mechanical *pressure* of the matrigel M . As *tumor cells are much larger than the chemoattractant molecules* we have $\mu_Q > \mu_C > \mu_U$. As we discussed above, tumor cells move towards positive gradients of both hetero and homotype chemoattractants, so we can write

$$\begin{aligned} \partial_t U = & \nabla[\mu_U(M) \nabla U] - \nabla[U \chi_Q(Q, M) \nabla Q] \\ & - \nabla[U \chi_C(C, M) \nabla C] + \lambda_U R_M(M, U), \end{aligned} \quad (6)$$

where λ_U is the inverse of the characteristic time of tumor

proliferation. Equations (1)–(6) constitute our reaction-diffusion tumor growth mathematical model.

III. ANALYTICAL STUDY

As we have stated above, the precise relevance of each of the factors summarized in Sec. II is not clearly understood. Partly, this is due to the complex interaction amongst these factors but, mainly, due to the lack of a systematic analytical and numerical analysis of each individual mechanism operating in the full system.

In this section, we analyze in detail every mechanism involved in tumor growth to determine which conditions trigger the formation of invasive branches, and how the interplay among those mechanisms allows these branches to be sustained in time.

A. Growth due to cell proliferation

Consider the subsystem of equations formed by Eqs. (1) and (6) with $\chi_Q = \chi_C = 0$, defined in a d -dimensional volume V . The tumor and nutrient *particles* are confined into the system and so the flux of material through the boundaries vanishes. This physical constraint introduces a conservation law in the problem, namely,

$$\frac{d}{dt} \int_V d\mathbf{x} (\lambda_M U + \lambda_U M) = 0, \quad (7)$$

independently of the precise functional form of the reaction term $R_M(M, U)$.

In the absence of diffusion ($\mu_M = \mu_U = 0$) this conservation law provides the following closed relation

$$M = K - \lambda_M / \lambda_U U, \quad (8)$$

where K depends on the initial conditions of M and U . If the diffusion coefficients do not vanish, we cannot obtain such closed relation between U and M , except in some simpler cases (related to the geometry of the volume and the initial conditions). With no loss of generality, we restrict ourselves to one and two-dimensional systems, $V=L$ and $V=L_x \times L_y$, respectively, and initial conditions such that $M(\mathbf{x}, t=0) = 0$ where $U(\mathbf{x}, t=0) \neq 0$ and $U(\mathbf{x}, t=0) = 0$ where $M(\mathbf{x}, t=0) \neq 0$. Then, we can obtain a relation similar to Eq. (8). Physically, this means that initially the nutrient surrounds the implanted tumor. In this case, Eq. (8) is valid after a small transient time (see Sec. IV), although the shape of the front (i.e., *surface of the tumor*) changes slightly. However, as we are interested in the case where tumor cells diffuse slowly, this front will be assumed to be sharp, and hence its exact shape is not relevant for our discussion below [13]. Thereby, we simply get

$$\partial_t U = \nabla[\mu_U(K - \lambda_M / \lambda_U U) \nabla U] + \lambda_U R_M(K - \lambda_M / \lambda_U U, U). \quad (9)$$

Tumor cells digest the matrigel nutrient when they are in direct contact. Thus, the reaction term $R_M(M, U)$ must vanish when any of its arguments does. The simplest choice of such a reaction term is $R_M(M, U) = MU$. Although other choices

are possible (leading qualitatively to the same results), we consider this choice to illustrate the main properties of the reduced system given by Eq. (9).

At this stage of the formal presentation, we need to consider separately the cases $\mu_M \ll \mu_U$ and $\mu_M \gg \mu_U$. Note that μ_U is M dependent so these inequalities need to be understood in an average sense.

1. $\mu_M \ll \mu_U$

We can define a *small* parameter $\varepsilon^2 = \mu_M / \mu_U$. As the diffusion coefficient of M is so small, the evolution of the density field M is slow in time, and therefore, random fluctuations in its initial condition remain at late times. Hence, the underlying medium is *quenched* from the perspective of the tumor cells. Moreover, these fluctuations take place on *fast* length scales, namely, we can write $\mu_U(M) \equiv \bar{\mu}_U(\mathbf{x}/\varepsilon)$ [32]. There are many studies devoted to the propagation of fronts in heterogeneous media (as is the case here for late times from the point of view of the tumor cells) [33]. Thus, it can be shown that, to leading order in ε , Eq. (9) can be assumed homogeneous. Namely, we can make the substitution

$$\bar{\mu}_U(\mathbf{x}/\varepsilon) \rightarrow \left\langle \frac{1}{\bar{\mu}_U} \right\rangle^{-1} \equiv \mu_U = \text{const} + O(\varepsilon), \quad (10)$$

where $\langle \dots \rangle$ denotes the average over a region of length l much greater than the characteristic length scale of the quenched fluctuations of M . This means that to lowest order we can assume a constant diffusion coefficient for U and that Eq. (9) becomes the well-known Fisher equation [34]. Fisher's equation admits planar traveling front solutions, with minimal wave speed v_0 given by [35]

$$v_0 = 2(\mu_U \lambda_U K)^{1/2}. \quad (11)$$

Moreover, any deviation from the planar front (or circular for two-dimensional tumors) damps out, so cell proliferation by itself cannot generate the branches observed in our experiments (see Fig. 1). Equation (11) provides the mean velocity of the tumor whenever proliferation is the only mechanism of tumor growth. However, chemotaxis drives tumor cells faster than proliferation itself, so v_0 is a small quantity. Thus, we can infer that cell proliferation is a long time process and consequently $\lambda_M \approx 0$ and $\lambda_U \approx 0$. We, therefore, assume that tumor cell proliferation is much slower than the chemotactically induced tumor cell growth (see Sec. III B).

Equation (10) is only valid to lowest order in ε . Corrections to the leading behaviour of μ_U provide also corrections to the velocity v_0 . It can be shown that [33]

$$v_0 = 2(\mu_U \lambda_U K)^{1/2} (1 + \xi^{1/2}), \quad (12)$$

where ξ is obtained from the expansion of $\mu_U(M)$ to first order in ε , and can be understood as a quenched noise term, i.e., a time independent random function [33]. Curvature corrections to Eq. (12) give the so-called quenched Kardar-Parisi-Zhang equation [36]. Thus, the heterogeneity of the matrigel medium will produce rough tumor interfaces. As we will see below, some tumor fluctuations (large length scales) are amplified by chemotaxis, so they act as *initial seeds* for invasive branches.

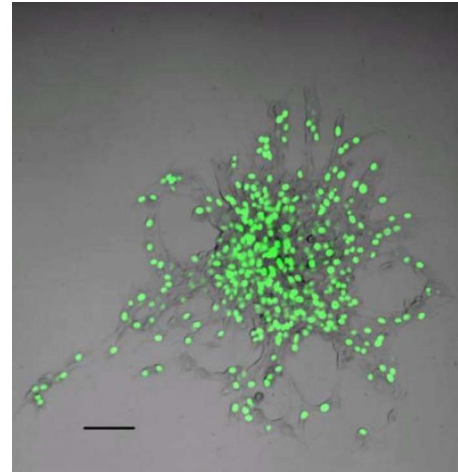


FIG. 1. (Color online) Depicted is an overlaid image of human U87 brain tumor cells which were stably transfected with a green fluorescent protein (EGFP) Histone 2B marker for nuclei. The image is taken from a central cross section of the MTS cultured in a three-dimensional extracellular matrix (Matrigel, Becton Dickinson, USA) environment *in vitro*. Note the chainlike invasive patterns. The image was taken one day post transferring the MTS from liquid medium to Matrigel (scale bar = 100 μm).

2. $\mu_M \gg \mu_U$

Despite the fact that the branching morphology in Fig. 1 has been obtained in the case $\mu_M \ll \mu_U$, for completeness, we include in this section the opposite limit as well.

In this limit the diffusion coefficient of M is so large that any fluctuation of M is rapidly damped out. In this case, we cannot clearly separate the regions where M takes its limiting values (0 and M_0), as was possible to do in the limit $\mu_M \ll \mu_U$ (see Fig. 2). In this case we have to deal with the full nonlinear equation that includes the dependence of μ_U on M . Hence, the specific form of the diffusion coefficient $\mu_U(M)$ is required in order to fully understand the evolution of the system. Müller and van Saarloos [37] have studied the specific case in which (in our notation) $\mu_U(K - \lambda_M / \lambda_U U) \sim U^k$, with $k > 0$. In such case, the gradient of the tumor field density U at the boundary of the tumor is discontinuous. This could be checked experimentally in order to determine the qualitative form of the diffusion coefficient $\mu_U(M)$.

B. Growth due to heterotype chemoattraction

In this paper we are interested in the case where the nutrient medium M diffuses slowly, and so the homogenization

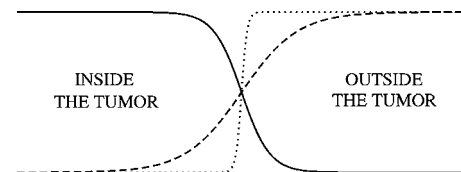


FIG. 2. M density field for the two limiting cases: $\mu_M \ll \mu_U$ (dotted line) and $\mu_M \gg \mu_U$ (dashed line). The solid line represents the density field of tumor cells U .

given by Eq. (10) can be assumed for all diffusion coefficients and chemotactic sensitivities. We, therefore, drop any dependence of these quantities on M . In what follows we restrict ourselves to a two-dimensional study, with no loss of generality (the three-dimensional analysis can be carried out as well).

As we have shown, cell proliferation cannot by itself provide invasive behavior. The next mechanism that we must include in order to understand cell invasion is heterotype chemoattraction, where the attractant molecules are provided externally to the tumor. They diffuse rapidly until they reach the tumor boundary and then two independent events take place: the heterotype chemoattractant is degraded by the tumor cells and the tumor cells are (*chemotactically*) drifted to higher heterotype chemoattractant concentration gradients.

The consumption rate of the heterotype chemoattractant, $R_Q(Q, U)$, cannot be arbitrarily large as it saturates for large values of Q . This assumption is based on the concept that each tumor cell carries a finite number of Q -uptaking cell receptors, which in turn determine the cell's maximum uptake rate. Besides, it is also a growing function of the tumor cell density, U . We do not need to specify the precise mathematical form of R_Q at this point, but taking into account the above assumptions, we can write, without loss of generality,

$$R_Q(Q, U) = U^\gamma f(Q), \quad (13)$$

with γ a positive constant.

In summary, the evolution equations in this case are

$$\partial_t U = \mu_U \nabla^2 U - \nabla [U \chi_Q(Q) \nabla Q], \quad (14)$$

and

$$\partial_t Q = \mu_Q \nabla^2 Q - a_Q U^\gamma f(Q), \quad (15)$$

where we have assumed that tumor cell proliferation is negligible compared to chemotaxis, so we can set $\lambda_M = \lambda_U = v_0 = 0$. In this limit the dynamics of M is uncoupled from that of Q and U .

Despite the fact that Eqs. (14) and (15) are highly nonlinear, due to the functions $\chi_Q(Q)$ and $f(Q)$, we can obtain useful information by properly rescaling space, time and both field densities Q and U . Thus, considering an initial tumor concentration U_0 located in a bounded region of the system and a replenished source of heterotype chemoattractant modeled by Eqs. (4), we define

$$\mathbf{x}' = \mathbf{x} \left(\frac{a_Q}{\mu_Q} \right)^{1/2}, \quad (16)$$

$$t' = t a_Q, \quad (17)$$

$$u = U/U_0, \quad (18)$$

$$q = Q/Q_0. \quad (19)$$

Equations (14) and (15) can be written (we drop primes for clarity) as follows

$$\partial_t u = \mu_U/\mu_Q \nabla^2 u - \nu Q_0/\mu_Q \nabla [u \bar{\chi}(q) \nabla q], \quad (20)$$

$$\partial_t q = \nabla^2 q - u^\gamma U_0^\gamma f(Q_0 q)/Q_0, \quad (21)$$

where $\bar{\chi}(q)$ is a dimensionless version of $\chi_Q(Q)$ and ν is defined through the relation

$$\nu \equiv \frac{\chi_Q(Q)}{\bar{\chi}(q)}. \quad (22)$$

Note that μ_Q is the fastest diffusivity in the problem, so we can define a small parameter $\epsilon = \mu_U/\mu_Q$. Moreover, we also assume that the *cross* diffusion coefficient νQ_0 is smaller than μ_Q [38]. With these considerations Eq. (20) becomes

$$\partial_t u = \epsilon \nabla^2 u - \rho \epsilon \nabla [u \bar{\chi}(q) \nabla q], \quad (23)$$

with $\rho = \nu Q_0/\mu_U$. Typically, the tumor field will be constant almost everywhere except in a narrow region (boundary layer [39]). This region defines an *interface* between the inside and the outside of the tumor.

In fact, if we take the limit $\epsilon \rightarrow 0$ (the so-called *outer limit* [39]) in Eq. (23), we have $\partial_t u = 0$, and

$$u = \begin{cases} 1 & \text{inside the tumor,} \\ 0 & \text{outside the tumor.} \end{cases} \quad (24)$$

One can see that in the outer limit the mathematical analysis of the problem is much simpler as Eq. (21) reduces to the equations

$$\partial_t q = \begin{cases} \nabla^2 q - U_0^\gamma f(Q_0 q)/Q_0 & \text{inside the tumor,} \\ \nabla^2 q & \text{outside the tumor.} \end{cases} \quad (25)$$

In the case $\epsilon \neq 0$ (the so-called *inner limit* [39]) we need to proceed with care: in order to solve Eq. (20) for u and Eq. (21) for q , we need the behavior of q exactly at the tumor boundary layer (interface). With this in mind, we define a new local set of curvilinear coordinates: a coordinate n normal to the tumor interface and a coordinate s tangential to it. Elementary computations (see Ref. [40]) give us the formulas for converting derivatives with respect to \mathbf{x} to derivatives with respect to the new coordinates (n, s) :

$$\nabla^2 = \partial_{nn} + \tilde{\kappa} \partial_n + \Delta_s, \quad (26)$$

where $\tilde{\kappa}$ is the local dimensionless curvature of the tumor interface and Δ_s is the surface Laplacian [40]. Similarly, we can write

$$\partial_t = \partial_t - \tilde{v} \partial_n + s_t \partial_s, \quad (27)$$

where \tilde{v} is the normal (dimensionless) velocity of the interface. We also need the following derivative:

$$\nabla [u \bar{\chi}(q) \nabla q] = \partial_n [u \bar{\chi}(q) \partial_n q] + \tilde{\kappa} [u \bar{\chi}(q) \partial_n q] + \nabla_s [u \bar{\chi}(q) \nabla_s q]. \quad (28)$$

Our aim now is to find solutions for q and u in the tumor interface. We start by rescaling the normal coordinate n , in terms of the fast variable $\eta = n/\epsilon$, and time in terms of $\tau = t/\epsilon$. We denote by \tilde{u} and \tilde{q} the *inner* fields, and expand them, $\bar{\chi}(\tilde{q})$ and \tilde{v} in a power series of ϵ [41]:

$$\tilde{u}(\eta, s, t) = \tilde{u}_0 + \epsilon \tilde{u}_1 + \dots, \quad (29)$$

$$\tilde{q}(\eta, s, t) = \tilde{q}_0 + \epsilon \tilde{q}_1 + \dots, \quad (30)$$

$$\tilde{v}(\eta, s, t) = \tilde{v}_0 + \epsilon \tilde{v}_1 + \dots, \quad (31)$$

$$\bar{\chi}(\tilde{q}) = \bar{\chi}(\tilde{q}_0) + \bar{\chi}'(\tilde{q}_0) \epsilon \tilde{q}_1 + \dots, \quad (32)$$

where the prime in Eq. (32) denotes a derivative with respect to \tilde{q} . Using Eqs. (23) and (26)–(28), the original system of equations can be written as

$$\begin{aligned} \partial_\tau \tilde{u}_0 + \epsilon \partial_\tau \tilde{u}_1 &= \epsilon \tilde{v}_1 \partial_\eta \tilde{u}_0 + \partial_{\eta\eta} \tilde{u}_0 + \epsilon \partial_{\eta\eta} \tilde{u}_1 - \epsilon s_t \partial_s \tilde{u}_0 + \epsilon \tilde{\kappa} \partial_\eta \tilde{u}_0 \\ &\quad - \rho \partial_\eta [\tilde{u}_0 \bar{\chi}(\tilde{q}_0) \partial_\eta \tilde{q}_0] - \epsilon \rho \partial_\eta [\tilde{u}_1 \bar{\chi}(\tilde{q}_0) \partial_\eta \tilde{q}_0] \\ &\quad - \epsilon \rho \partial_\eta [\tilde{u}_0 \bar{\chi}'(\tilde{q}_0) \partial_\eta \tilde{q}_1] - \epsilon \rho \partial_\eta [\tilde{u}_0 \bar{\chi}'(\tilde{q}_0) \tilde{q}_1 \partial_\eta \tilde{q}_0] \\ &\quad - \epsilon \rho \tilde{\kappa} \tilde{u}_0 \bar{\chi}'(\tilde{q}_0) \partial_\eta \tilde{q}_0 + O(\epsilon^2), \end{aligned} \quad (33)$$

$$\epsilon \partial_\tau \tilde{q}_0 = \partial_{\eta\eta} \tilde{q}_0 + \epsilon \partial_{\eta\eta} \tilde{q}_1 + \epsilon \tilde{\kappa} \partial_\eta \tilde{q}_0 + O(\epsilon^2). \quad (34)$$

1. Order ϵ^0

We start by solving Eqs. (33) and (34) to order ϵ^0 . As we stated above, tumor cell proliferation is negligible when compared to chemotaxis, which means that $\tilde{v}_0 = 0$. Otherwise we have to include the reaction term R_M in the dynamical equation for U and then, to order ϵ^0 , Eq. (33) becomes

$$\begin{aligned} \partial_\tau \tilde{u}_0 + \epsilon \partial_\tau \tilde{u}_1 &= \tilde{v}_0 \partial_\eta \tilde{u}_0 + \epsilon \tilde{v}_1 \partial_\eta \tilde{u}_0 + \epsilon \tilde{v}_0 \partial_\eta \tilde{u}_1 + \partial_{\eta\eta} \tilde{u}_0 + \epsilon \partial_{\eta\eta} \tilde{u}_1 \\ &\quad - \epsilon s_t \partial_s \tilde{u}_0 + \epsilon \tilde{\kappa} \partial_\eta \tilde{u}_0 - \rho \partial_\eta [\tilde{u}_0 \bar{\chi}(\tilde{q}_0) \partial_\eta \tilde{q}_0] \\ &\quad - \epsilon \rho \partial_\eta [\tilde{u}_1 \bar{\chi}(\tilde{q}_0) \partial_\eta \tilde{q}_0] - \epsilon \rho \partial_\eta [\tilde{u}_0 \bar{\chi}'(\tilde{q}_0) \partial_\eta \tilde{q}_1] \\ &\quad - \epsilon \rho \partial_\eta [\tilde{u}_0 \bar{\chi}'(\tilde{q}_0) \tilde{q}_1 \partial_\eta \tilde{q}_0] - \epsilon \rho \tilde{\kappa} \tilde{u}_0 \bar{\chi}'(\tilde{q}_0) \partial_\eta \tilde{q}_0 \\ &\quad + \epsilon \frac{\lambda_U K}{a_Q} \left(1 - \frac{\lambda_M U_0}{\lambda_U K} \right) \tilde{u}_0 + O(\epsilon^2). \end{aligned} \quad (35)$$

Notice that in the absence of chemotaxis Eq. (35) becomes Fisher's equation in the set of coordinates (η, s) and with time given by τ .

From Eq. (34) we find

$$\partial_{\eta\eta} \tilde{q}_0 = 0. \quad (36)$$

We know that \tilde{q}_0 must be bounded at $\eta = \pm\infty$, corresponding to the inside and outside of the tumor in the scaled variable η . This implies $\partial_\eta \tilde{q}_0 = 0$ and, therefore, $\tilde{q}_0 = \text{constant}$. Substituting this into Eq. (33), we obtain

$$\partial_\tau \tilde{u}_0 = \partial_{\eta\eta} \tilde{u}_0, \quad (37)$$

which states the fact that, to first order, the tumor cells simply diffuse. Note that to this order \tilde{u}_0 does not depend on s , so that $\partial_s \tilde{u}_0 = 0$, due to the boundary conditions on u .

2. Order ϵ^1

To next order in ϵ and from Eq. (34) we find,

$$\partial_{\eta\eta} \tilde{q}_1 = 0 \Rightarrow \partial_\eta \tilde{q}_1 = \text{const}, \quad (38)$$

due to the boundary conditions on q .

The next order equation for \tilde{u}_1 is given by

$$\partial_\tau \tilde{u}_1 = \tilde{v}_1 \partial_\eta \tilde{u}_0 + \partial_{\eta\eta} \tilde{u}_1 + \tilde{\kappa} \partial_\eta \tilde{u}_0 - \rho (\partial_\eta \tilde{u}_0) \bar{\chi}'(\tilde{q}_0) \partial_\eta \tilde{q}_1. \quad (39)$$

The Fredholm alternative (or solvability condition) for \tilde{u}_1 provides [41]

$$\tilde{v}_1 = -\tilde{\kappa} + \rho B \partial_\eta \tilde{q}_1, \quad (40)$$

where

$$B = \frac{\int_{-\infty}^{\infty} d\eta (\partial_\eta \tilde{u}_0)^2 \bar{\chi}(\tilde{q}_0)}{\int_{-\infty}^{\infty} d\eta (\partial_\eta \tilde{u}_0)^2}. \quad (41)$$

Matching the inner and outer expansions yields the normal velocity of the tumor in the original dimensions [41]

$$v_n = -\mu_U \kappa + \nu B \nabla Q \cdot \mathbf{n}, \quad (42)$$

where κ is the mean curvature of the level surfaces of constant normal coordinate, ν has been defined in Eq. (22) and \mathbf{n} is a unit vector normal to the tumor interface and directed away from the tumor.

Chemotactically induced tumor growth requires $\nabla Q \cdot \mathbf{n}$ to be a positive quantity, so that v_n is positive. This can be achieved whenever the heterotype chemoattractant concentration grows as we move away from the tumor surface. Before performing the analysis of Eqs. (25) and (42) to check this requirement, we consider two interesting features related to Eq. (42). First of all, in the absence of chemotaxis and proliferation, for an initially circular tumor of radius R_0 , Eq. (42) reduces to

$$\frac{dR}{dt} = -\frac{\mu_U}{R}, \quad (43)$$

where we have made use of the following facts: for circular tumors the normal coordinate n is the radius R , so that $v_n = dR/dt$; the mean curvature of a surface of constant R is $\kappa = 1/R$; and in the absence of chemotaxis $\nu = 0$. Equation (43) gives the diffusive behavior $R(t) = \sqrt{R_0^2 - 2\mu_U t}$. This means that the mean velocity of the tumor due to diffusion decays as $t^{-1/2}$. At this stage, and for an initially circular tumor, one could now perform the following analysis: (i) suppose the tumor continues to grow as a two-dimensional disk and (ii) perturb the boundary and study the development of instabilities. This is out of the scope of this paper and will be addressed in future work. Second, for a general tumor front geometry, Eq. (42) provides a critical curvature, (reminiscent of the classical Greenspan model [13])

$$\kappa_c = \frac{\nu B}{\mu_U} \nabla Q \cdot \mathbf{n}, \quad (44)$$

such that for $\kappa < \kappa_c$ the tumor interface has locally a positive velocity, for $\kappa > \kappa_c$ the tumor interface has locally a negative velocity and for $\kappa = \kappa_c$ the tumor interface has locally vanishing velocity. Note that this is precisely the reason of the dynamical instability that guarantees the development of invasive branches. Tumor invasion will take place on the tumor surface wherever the local curvature is below the critical

value κ_c , given by Eq. (44). Our result agrees with the specific case considered in Ref. [17].

As a final remark concerning Eq. (42), note that it resembles the equation for the velocity of a solidification front [42,43]. In that case, the local normal velocity of the front depends on the local curvature, κ as above, but on the value of the field (temperature) at the boundary, instead of the value of the gradient, ∇Q , at the tumor interface. This is to be expected as in the tumor picture it is the heterotype chemoattractant that is driving the dynamics, and in the case of a solidification front, the dynamics of the front is linked to the temperature field [42,43]. The branching behavior of the tumor also resembles the fingering instability of the Hele-Shaw problem [44].

We now turn to the requirement on the value of $\nabla Q \cdot \mathbf{n}$. In order to check that, indeed, $\nabla Q \cdot \mathbf{n}$ (or equivalently $\nabla q \cdot \mathbf{n}$) is a positive quantity at the tumor boundary, we need to solve Eq. (25) supplemented by Eq. (42), with the initial condition

$$q(x,y,t=0) = \delta(x - L_x), \quad (45)$$

and boundary conditions

$$q(x=0,y,t) = 0, \quad (46)$$

$$q(x=L_x,y,t) = 1. \quad (47)$$

These equations cannot be solved in general without the precise form of the function $f(Q)$. Nevertheless, we may assume that, as tumor cells degrade the heterotype chemoattractant, the concentration of q inside the tumor is small enough, and we can approximate $f(Q)$ by a linear function $f(Q_0q) \approx \delta q$. We now proceed by solving Eq. (25) inside and outside the tumor (we denote the solutions, respectively, by q^- and q^+) and matching both solutions at the boundary, for an initially flat tumor, i.e., a tumor for which the radius of curvature is much smaller than the system lateral size L_x [45]. We first notice that q^+ is invariant under the transformation group $(L_x - x) \rightarrow \epsilon(L_x - x), t \rightarrow \epsilon^2 t$ and $q^+ \rightarrow \epsilon^0 q^+$. Similarly, $e^{\delta t} q^-$ is invariant under the group, $x \rightarrow \epsilon x, t \rightarrow \epsilon^2 t$ and $q^- \rightarrow \epsilon^0 q^-$. Thus, it can be straightforwardly seen that [46]

$$q^-(x,y,t) = C e^{-\delta t} \int_0^{x/\sqrt{t}} d\xi e^{-\xi^2/4}, \quad (48)$$

$$q^+(x,y,t) = 1 - A \int_0^{(L_x-x)/\sqrt{t}} d\xi e^{-\xi^2/4}, \quad (49)$$

where A and C are positive constants that can be determined by continuity of the solutions at the tumor boundary $\mathbf{x} = \mathbf{x}_0(s,t)$. As we are interested in the gradient of the Q density field, we find

$$\partial_x q^-(x,y,t) = \frac{C}{\sqrt{t}} e^{-\delta t} e^{-x^2/4t}, \quad (50)$$

$$\partial_x q^+(x,y,t) = \frac{A}{\sqrt{t}} e^{-(L_x-x)^2/4t}. \quad (51)$$

Note that Eq. (51) states that the gradient of Q is a positive function, and so the tumor velocity is increased by chemot-

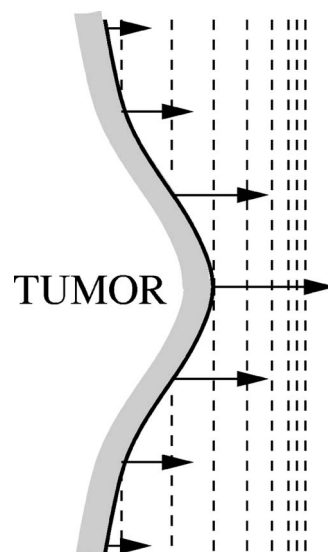


FIG. 3. Sketch of the heterotype chemoattractant effect on tumor cell invasive drift. Dashed lines represent level sets of Q and arrows represent the local normal velocity of the tumor cells due to chemotaxis (the length of the arrows is proportional to the normal velocity).

axis as we had anticipated. Moreover, the larger the distance from x to the tumor is, the larger the value of $\partial_x q^+$ becomes and the larger the value of the velocity front is (see Fig. 3). This is indeed, the reason why small fluctuations on the tumor surface become emerging invasive branches. We will see in Sec. IV that this chemotactically enhanced velocity is also obtained numerically.

C. Growth due to homotype chemoattraction

Finally, we consider the role of homotype chemoattractants. Representing protein growth factors, these chemoattractants are produced and internalized [47], or (for the purposes here), consumed by the tumor cells that move towards their positive gradients, in a similar fashion as in the heterotype case. Yet, there is no wide time scale separation between tumor and homotype chemoattractant dynamics. Thus, we cannot, in general, neglect tumor cell proliferation when analyzing homotype chemoattractant dynamics. This means that the equations in this case are Eqs. (1), (5), and (6) with $\chi_Q = 0$. Performing a similar analysis to that of Sec. III B above we find:

$$v_n = 2(\mu_U \lambda_U K)^{1/2} - \mu_U \kappa + v' B' \nabla C \cdot \mathbf{n}. \quad (52)$$

Despite the fact that Eq. (52) is equivalent to Eq. (42), the main differences between the evolution of Q and C are due to the behavior of both density fields away from the tumor interface, namely, due to the production term $R_C^{(p)}$ (that is absent in the dynamical equation for Q) and the different boundary conditions (no external source for C).

Following the same steps as those carried out in Sec. III B, we find that the *outer* limit yields the following equation:

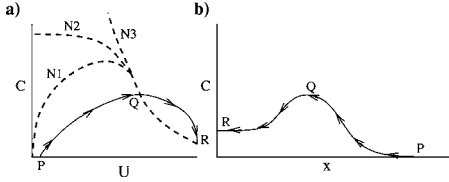


FIG. 4. (a) Qualitative behavior of the *trajectory* of the density field C in the *phase plane*. The arrows indicate the direction of time evolution. Curves $N1$ – $N3$ are the three types of nullclines that can be expected for our system. (b) Same trajectory of the density field C with respect to the spatial coordinate x . Again, arrows indicate time evolution.

$$\partial_t c = \begin{cases} \nabla^2 c + r^{(p)}(0,1) - r^{(d)}(c,1) & \text{inside the tumor,} \\ \nabla^2 c & \text{outside the tumor,} \end{cases} \quad (53)$$

with $r^{(p)}$ and $r^{(d)}$ scaled (dimensionless) versions of $R_C^{(p)}$ and $R_C^{(d)}$, respectively. Note that we have considered $m=0$ where $u=1$. The conservation relation given by Eq. (8) still holds in this case so, without loss of generality, we reduce the system of Eqs. (1), (5), and (6) to Eqs. (5) and (6), with $\chi_Q=0$ and M given by Eq. (8).

Just as we did in Sec. III B, we must now compute the sign of $\nabla C \cdot \mathbf{n}$ in order to determine whether or not homotype chemotaxis increases the velocity of the tumor boundary, and if it can generate a dynamical instability leading to a tumor branching morphology. We cannot in general find a transformation group under which Eq. (53) is invariant. This means that we cannot study homotype chemotaxis with the tools of the previous section. However, we can analyze homotype chemoattraction by means of its homogeneous and steady state solutions, based on generic assumptions regarding the reaction terms $R_C^{(p)}(M, U)$ and $R_C^{(d)}(C, U)$.

The homogeneous, steady state solutions (nullclines [48]) of Eqs. (5) and (9) are given by the solutions of

$$R_M(K - \lambda_M/\lambda_U U, U) = 0, \quad (54)$$

$$R_C^{(p)}(K - \lambda_M/\lambda_U U, U) = R_C^{(d)}(C, U). \quad (55)$$

These nullclines yield the fixed points $U_1=0$ and $U_2 = \lambda_U K/\lambda_M$, and C_1 and C_2 given implicitly by Eq. (55). We must distinguish between the inside and the outside of the tumor when analyzing tumor growth due to homotype chemotaxis. Outside the tumor $U_1=0$ and there is no production of C (as there are no tumor cells). This implies that the corresponding fixed point value of C is then $C_1=0$. On the other hand, inside the tumor, Eq. (55) reflects the fact that there is a balance between production and consumption of C . This means that the value of the density field C reaches the fixed point C_2 , which is a constant (equilibrium) value. This simple picture holds even far enough from the tumor boundary (diffusion tends to spread these uniform concentration phases). Therefore, let us consider a point in the C – U plane where $U=U_p$ and $C=0$ [point P in Fig. 4(a)], namely, a point outside the tumor boundary, with U so small that there has been no previous secretion of homotype chemoattractant C .

The concentration C eventually grows (as U increases due to proliferation wherever $M \neq 0$) because the slope given by

$$\frac{dC}{dU} = \frac{R_C^{(p)}(K - \lambda_M/\lambda_U U, U) - R_C^{(d)}(C, U)}{R_M(K - \lambda_M/\lambda_U U, U)}, \quad (56)$$

is positive [49]. Then, the slope decreases [50] until it reaches the nullcline where the slope is 0 [point Q in Fig. 4(a)]. Finally, the curve approaches the stable point (U_2, C_2) with infinite slope [point R in Fig. 4(a)]. Thus, C grows from the outside of the tumor, reaches a maximum value and then decreases to a constant value C_2 inside the tumor. This can be schematically seen in Fig. 4(b). In other words, the density field C tends to grow as U decreases namely, as we move outside of the tumor from inside. But, as we have shown, outside the tumor and far enough from it C tends to 0. This means that C also tends to grow as we move inside of the tumor from the outside. Consequently, C behaves as a pulse from the constant value C_2 inside the tumor to $C_1=0$ outside the tumor. This qualitative picture is sketched in Fig. 4, where we have shown that the nullcline given by Eq. (55) can have three different qualitative behaviours N_1, N_2 and N_3 , that are plotted as well. This pulslike structure for the density profile of C agrees well with the intuitive picture provided in Sec. II C. It also explains why tumor cells are chemotactically guided by the gradient of C . These facts will be numerically confirmed in Sec. IV below. We conclude as follows: the density profile of C grows at the tumor boundary, which implies that the local normal velocity of the tumor surface increases due to the presence of a positive homotype chemoattractant gradient.

IV. NUMERICAL STUDY

In Sec. III we have presented a general analytical framework to study tumor growth (proliferation and chemotactic invasion). The previous analysis has been carried out by means of several assumptions and limits (e.g., $\nu Q_0 \ll \mu_Q, \lambda_M \approx 0, \lambda_U \approx 0$) that have not been fully justified. In this section we provide numerical simulations that check the validity of those assumptions and limits. We, thus, numerically solve the main differential equations of Sec. II following a similar organization to that of Sec. III. It is clear that in order to carry out a numerical study we must specify the detailed mathematical form of the reaction terms in our Eqs. (1)–(6). These reaction terms are chosen following the spirit of the oncology concept previously reported in Refs. [8,23].

There exists a vast literature on computational methods applied to moving boundary problems for tumor growth, see for example Ref. [51]. We have used a fourth order Runge-Kutta method of integration. We have also made use of different time steps and the results do not change significantly from the ones shown in the figures.

A. Growth due to cell proliferation

In this section, we check the validity of Eq. (8) as an approximation to Eq. (7). Thus, we have integrated Eqs. (1) and (6) with $\chi_Q = \chi_C = 0$ and $R_M(U, M) = MU$ and, independently, Eq. (6) with $M = K - \lambda_M/\lambda_U U$.

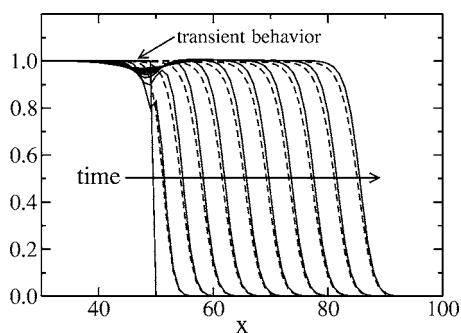


FIG. 5. One-dimensional tumor proliferation. Solid lines represent the U density field for the model given by Eqs. (1) and (6). Dashed lines represent U for the solution of Fisher's equation, i.e., Eq. (6) with $M=K-\lambda_M/\lambda_U U$.

1. One-dimensional results

Initially, we place a *one-dimensional tumor* such that $U(x,t=0)=1$ for $0 < x < L/2$ and $U(x,t=0)=0$ elsewhere. This implies that at the initial time $M(x,t=0)=1-U(x,t=0)$. We have numerically solved Eqs. (1) and (6) with $\chi_Q=\chi_C=0$ and $R_M(U,M)=MU$ and, independently, Eq. (6) with $M=K-\lambda_M/\lambda_U U$. The lattice separation has been taken $dx=0.5$, the lattice size $L_x=128$, the diffusion coefficients $\mu_U=0.01$ and $\mu_M=0.0$, the reaction rates $\lambda_M=\lambda_U=0.1$, the time step $\epsilon_t=0.005$, the initial time $t_0=\epsilon_t$ and the final time $t_f=50\,000\epsilon_t$.

As can be seen in Fig. 5, after a small transient time, the approximation is accurate enough. As we mentioned in Sec. III, the shape of the tumor front changes slightly.

2. Two-dimensional results

We now consider tumor growth due to proliferation in a two-dimensional setting with $\chi_Q=\chi_C=0$. Initially, the matrigel density M is a random distribution to reflect the fact that it is an heterogeneous medium. As we are interested in a slowly varying nutrient, we choose $\epsilon \equiv \mu_M/\bar{\mu}_U=0.01$, where $\bar{\mu}_U$ is the maximum attainable value of $\mu_U(M)$. We assume that this value of μ_U corresponds to the value $M=0$. The confinement due to the matrigel is unlimited, namely, for large concentrations of M , tumor cells can no longer diffuse. Hence, we take the following diffusion coefficient :

$$\mu_U(M) = \frac{\bar{\mu}_U}{1 + M/M_{\text{th}}}, \quad (57)$$

where M_{th} is a reference threshold concentration.

We have solved Eqs. (1) and (6) with the following initial conditions: at time $t=0$ we place a circular tumor centered at $(L_x/2, L_y/2)$ of radius $L_x/4$ and surrounded by a heterogeneous nutrient substrate M . Thus, $M(x,y,t=0)=0$ inside the initial circular tumor and $M(x,y,t=0)=1+\xi(x,y)$ elsewhere, with $\xi(x,y)$ a random Gaussian distribution with zero mean and variance 0.2, that encodes the initial heterogeneities of the matrigel. The lattice separation has been taken $dx=dy=0.5$, the lattice size $L_x=L_y=128$, the diffusion coefficients $\bar{\mu}_U=0.01$ and $\mu_M=0.0$, the reaction rates $\lambda_M=\lambda_U=1.5$, the time step $\epsilon_t=0.005$, the initial time $t_0=\epsilon_t$, the final time t_f

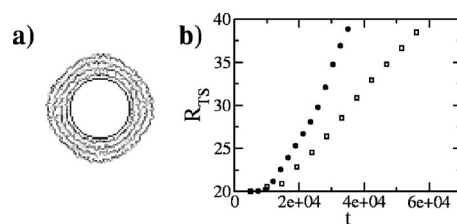


FIG. 6. (a) Numerical simulation of an initially circular tumor embedded in a matrigel medium M with slow dynamics ($\mu_M \ll \bar{\mu}_U$). Different curves represent different times with the initial time t_0 corresponding to the inner perfect circle. (b) Time evolution of the tumor spheroid average radius, R_{TS} , for $\mu_U=0.01$, $\mu_Q=10$, $\mu_M=0.000\,01$, $\lambda_M=0.05$, $a_Q=0.75$, $b_Q=0.5$ and $\chi_Q=0$ (squares) and $\chi_Q=2$ (solid circles).

$=5000\epsilon_t$, and the intermediate times (1000, 2000, 3000, 4000) ϵ_t .

Figure 6(a) displays the time evolution of the tumor surface. Notice how the tumor conserves during its evolution its initial circular shape but develops a rough interface with the matrigel. In Fig. 6(b) we show the time evolution of the tumor spheroid average radius (defined accordingly to Ref. [8]) when the heterotype chemoattractant (see next section) is both absent and present. Note that chemotaxis is a crucial ingredient in the fast invasion of tumor cells.

B. Growth due to heterotype chemoattraction

The experimental branches of Fig. 1 have two characteristic lengths, namely, their width and their height with respect to the main tumor substrate. Section III B was devoted to determine the conditions that trigger the formation of the invasive branches. We know that the height of the branches depends in a crucial way on the mathematical form of the reaction term $R_Q(Q,U)$ of Eq. (2), namely, the height depends on the concentration thresholds associated with the biochemical reaction of Q consumption by tumor cells [8]. Thus, we choose

$$a_Q R_Q(Q,U) = a_Q U \frac{Q}{b_Q + Q}, \quad (58)$$

where a_Q is the inverse of the time scale of consumption and b_Q a characteristic heterotype chemoattractant concentration (threshold value). Note that, in the notation of Eq. (15) we have set $\gamma=1$.

Two-dimensional results

We have integrated Eqs. (1), (2), and (6) with R_Q given by Eq. (58) and $\chi_C=0$. At the initial time we place a circular tumor at $(L_x/2, L_y/2)$ with radius $L_x/4+\xi$, where ξ is a Gaussian random number with zero mean and variance $L_x/20$. This initial condition mimics the effect of the slowly varying underlying substrate (matrigel) as shown in the previous Sec. IV A. The lattice separation has been taken $dx=dy=0.5$, the lattice size $L_x=L_y=128$, the diffusion coefficients $\mu_U=0.001$, $\mu_Q=10.0$ and $\mu_M=0.000\,01$, the reaction rates $\lambda_M=\lambda_U=0.0050a_Q=0.75$, $b_Q=0.5$, the chemotactic sen-

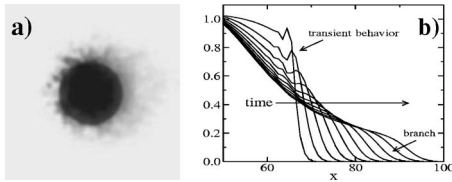


FIG. 7. (a) Numerical simulation of tumor branching induced by a heterotype chemotactic source located at $x=L_x$. The plot represents the tumor density field $U(x,y,t=20\,000\epsilon_t)$. (b) Cross section of the tumor in panel (a) for different times between $2000\epsilon_t$ and $20\,000\epsilon_t$.

sitivity $\chi_Q=2.0$, the time step $\epsilon_t=0.005$, the initial time $t_0=\epsilon_t$, and the final time $t_f=20\,000\epsilon_t$.

Figure 7(a) displays the numerically obtained tumor when the replenished source of Q is placed at $x=L_x$ (i.e., the right hand side of the lattice). Moreover, in Fig. 7(b) we show the cross section of an invasive, chemotactically induced branch obtained in the same simulation. Clearly, we can distinguish between the main tumor spheroid and a given branch. Notice the good agreement with the experimental results and with the qualitative analysis provided in Sec. III.

C. Growth due to homotype chemoattraction

The segregation and eventual degradation of the homotype chemoattractant is limited, i.e., the rates associated with both processes cannot be arbitrarily large. Thus, following Ref. [23] we choose

$$\alpha_C R_C^{(p)}(U) = \alpha_C \frac{U}{\beta_C + U}, \quad (59)$$

$$a_C R_C^{(d)}(C, U) = a_C U \frac{C}{b_C + C}. \quad (60)$$

The constants α_C and a_C are the inverse of the characteristic time scales of production and degradation, respectively, and β_C and b_C are characteristic saturation concentrations (for production and degradation, respectively). Note the Eqs. (60) and (58) have the same mathematical form.

Two-dimensional results

We have numerically integrated Eqs. (1), (5), and (6) with $\chi_Q=0$, and $R_C^{(p)}$ and $R_C^{(d)}$ given by Eqs. (59) and (60), respectively. The initial conditions for $U(x,y,t=0)$ are the same as those chosen in the previous Sec. IV B. For the matrigel and the homotype chemoattractant, we have chosen $M(x,y,t=0)=1-U(x,y,t=0)$ and $C(x,y,t=0)=0$, respectively. The lattice separation has been taken $dx=dy=0.5$, the lattice size $L_x=L_y=128$, the diffusion coefficients $\mu_U=0.01$, $\mu_C=1.0$, and $\mu_M=0.0$, the reaction rates $\lambda_M=\lambda_U=0.1$, $a_C=1.75$, $b_C=0.1$, $\alpha_C=\beta_C=1.0$, the chemotactic sensitivity $\chi_C=1.0$, the time step $\epsilon_t=0.005$, the initial time $t_0=\epsilon_t$, and the final time $t_f=50\,000\epsilon_t$.

Figure 8 displays the time evolution of the tumor profile in the x direction for times $10\,000\epsilon_t$, $15\,000\epsilon_t$, $20\,000\epsilon_t$, $25\,000\epsilon_t$, and $30\,000\epsilon_t$. The dotted line in Fig. 8

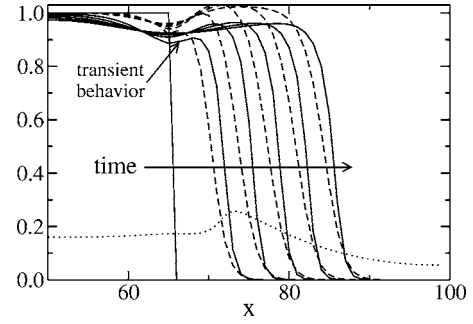


FIG. 8. Cross section of a tumor for the case of coupled dynamics between matrigel M , tumor cells U and homotype chemoattractant C for different times between $t_0=\epsilon_t$ and $t_f=30\,000\epsilon_t$. Solid lines: U subject to homotype chemotaxis; dashed lines: U subject to no homotype chemotaxis. Dotted line: C (times a factor of four) for $t=10\,000\epsilon_t$.

displays the C profile at time $t=10\,000\epsilon_t$, magnified by a factor of 4. In agreement with the analysis presented in Sec. III C, the numerical results show that (i) there is no emergence of chemotactically induced branches, as was the case for the heterotype chemoattractant and (ii) the mean speed of the tumor boundary increases due to C . That is, the tumor profile follows qualitatively the behavior anticipated in Sec. III C.

V. DISCUSSION AND CONCLUSIONS

In summary we conclude that:

(1) The matrigel M induces tumor cell proliferation. This growth is an overall expansion of the initial tumor that follows the principle of *least resistance* [23]. Moreover, in the case of interest here, that of a slowly diffusing matrigel, the tumor boundary (or surface) becomes inhomogeneous due to the random nature of the slowly varying nutrient M . It is noteworthy that the roughness of the tumor surface depends also on the proliferation rate of the cells.

(2) The homotype chemoattractant enhances the velocity of the tumor cells due to the increase of C at the boundary of the tumor. This effect combined with cell proliferation (due to M) would induce the onset of invasion of tumor cells towards regions of lower matrigel density. We have been able to show that the secretion and subsequent diffusion of C catalyzes the motion of the tumor cells.

(3) Finally, as the heterotype chemoattractant is introduced into the system at a given distance from the tumor (in our case at the boundary), and because it diffuses, an initially circular tumor develops unstable invasive branches that move towards the source of the heterotype chemoattractant. These branches develop from *initial seeds* (i.e., fluctuations on the tumor boundary), which are due to the mechanical confinement from M , and the velocity enhancement due to C and Q .

Our results are an improvement over Ref. [7,23]. We have not limited ourselves to (i) performing a linear stability analysis from the steady state solutions as was done in Ref. [7] or to (ii) numerically solving a simplified version of the reaction-diffusion equations as carried out in Ref. [23]. On

the other hand, we have analytically and numerically studied the full nonlinear problem. The simplicity of the model allows the analytic treatment introduced in Sec. III; indeed, this is a very useful result as it visualizes a variety of interesting phenomena. Yet, the same analysis may not be applied to a relatively more sophisticated model. The results of the work presented here allow us to say that proliferation is a requirement for invasion. In fact, there can be no (chemotactic) invasion without proliferation, as proliferation due to M provides the initial seeds that trigger the onset of invasion. That is, the slow diffusion of M is crucial to the development of those initial seeds (rough tumor interface) that become invasive branches due to heterotype chemotactically induced instability.

Admittedly, our model still does have several shortcomings as it inevitably has to simplify the complex biological scenario considered here. For instance, tumor cell apoptosis and thus, the development of a central necrotic core is currently not included [31]. Incorporating this characteristic tumor feature would also have implications for the simulation itself. Specifically, detrimental byproducts released from the dying virtual cells would render this area “toxic,” resulting in a central space within the growing tumor, which is not being repopulated by the proliferative tumor surface. In future work, this tumor characteristic can be implemented, e.g., by some dynamic, internal boundary condition within the tumor. We have not yet considered the finite receptor occupancy of the tumor cell surface. This issue is important in order to find biological support for implementing a maximum threshold of (e.g., homotype) chemoattractant uptake rate (by each tumor cell). On the other hand, the minimum threshold is given by the maximum sensitivity of the cell surface-based receptor

system. Nonetheless, even in its present form the model already proves very useful for interdisciplinary cancer research as it provides the following, at least in part experimentally testable hypotheses: (i) tumor cell proliferation by itself cannot generate the invasive branching behavior observed experimentally, yet, proliferation is a requirement for invasion, (ii) heterotype chemotaxis provides an instability mechanism that leads to the onset of tumor cell invasion, and (iii) homotype chemotaxis does not provide such a mechanism but enhances the mean speed of the tumor surface.

Combined with more specific experimental data, both on the molecular and on the microscopic scale, this ongoing work may therefore reveal exciting insights into the role of tumor cell signaling and its impact on the emergence of multicellular patterns.

ACKNOWLEDGMENTS

C.M.-P. and T.S.D. would like to thank S. Habib (Los Alamos National Laboratory) for very valuable discussions. C.M.-P. would like to thank B. D. Sleeman (University of Leeds) for a very careful reading of the manuscript and for useful discussions. This work has been partially supported by MECD (Spain) Grant No. BFM2003-07749-C05-05. T.S.D. would like to acknowledge support by NIH Grants Nos. CA 085139 and CA 113004 and by the Harvard-MIT (HST) Athinoula A. Martinos Center for Biomedical Imaging and the Department of Radiology at Massachusetts General Hospital. We thank C. Athale (Complex Biosystems Modeling Laboratory, Massachusetts General Hospital) for providing the microscopy image.

-
- [1] C. Betsholtz, B. Westermark, B. Ek, and C. H. Heldin, *Cell* **39**, 447–57 (1984).
- [2] J. Laterra, E. Rosen, M. Nam, S. Ranganathan, K. Fielding, and P. Johnston, *Biochem. Biophys. Res. Commun.* **235**, 743 (1997).
- [3] M. R. Chicoine, C. L. Madsen, and D. L. Silbergeld, *Neurosurgery* **36**, 1165 (1995).
- [4] M. J. Plank, B. D. Sleeman, and P. F. Jones, *Theor. Med.* **4**, 251 (2002); M. J. Plank and B. D. Sleeman, *Bull. Math. Biol.* **66**, 1785 (2004).
- [5] S. Koochekpour, M. Jeffers, S. Rulong, G. Taylor, E. Klineberg, E. A. Hudson, J. H. Resau, and G. F. Vande Woude, *Cancer Res.* **57**, 5391 (1997); A. J. Ekstrand, C. D. James, W. K. Cavenee, B. Seliger, R. F. Pettersson, and V. P. Collins, *ibid.* **51**, 2164 (1991).
- [6] A. Wells, *Adv. Cancer Res.* **78**, 31 (2000).
- [7] L. M. Sander and T. S. Deisboeck, *Phys. Rev. E* **66**, 051901 (2002).
- [8] T. S. Deisboeck, M. E. Berens, A. R. Kansal, S. Torquato, A. O. Stemmer-Rachamimov, and E. A. Chiocca, *Cell Prolif.* **34**, 115 (2001).
- [9] R. B. Vernon and E. H. Sage, *Microvasc. Res.* **57**, 118–133 (1999).
- [10] H. M. Byrne and M. A. J. Chaplain, *Eur. J. Appl. Math.* **8**, 639 (1998).
- [11] T. L. Jackson, S. R. Lubkin, and J. D. Murray, *J. Math. Biol.* **39**, 353 (1999).
- [12] L. Derbel, *Math. Models Meth. Appl. Sci.* **14**, 1657 (2004); E. De Angelis and P. E. Jabin, *ibid.*, **13**, 187 (2003).
- [13] H. Greenspan, *J. Theor. Biol.* **56**, 229 (1976).
- [14] J. P. Ward and J. R. King, *IMA J. Math. Appl. Med. Biol.* **14**, 39 (1997).
- [15] M. J. Holmes and B. D. Sleeman, *J. Theor. Biol.* **202**, 45 (2000).
- [16] T. Alarcon, H. Byrne, and P. Maini, *J. Theor. Biol.* **229**, 395 (2004).
- [17] D. S. Jones and B. D. Sleeman, *Differential Equations and Mathematical Biology* (CRC Press, London, 2003), and references therein.
- [18] H. Levine, S. Pamuk, B. Sleeman, and M. Nilsen-Hamilton, *Bull. Math. Biol.* **63**, 801 (2001).
- [19] H. Levine, S. Pamuk, B. Sleeman, and M. Nilsen-Hamilton, *J. Math. Biol.* **42**, 195 (2001).
- [20] N. Bellomo, E. De Angelis, and L. Preziosi, *Theor. Med.* **5**, 111 (2003).
- [21] N. Bellomo, A. Bellouquid, and M. Delitala, *Math. Models*

- Meth. Appl. Sci. **14**, 1683 (2004).
- [22] Z. Bajzer and S. Vuk-Pavlovic, *BioSystems* **80**, 1 (2005).
- [23] S. Habib, C. Molina-París, and T. S. Deisboeck, *Physica A* **327**, 501 (2003).
- [24] E. F. Keller, and L. A. Segel, *J. Theor. Biol.* **30**, 225 (1971); **30**, 235 (1971).
- [25] J. A. Sherratt, *Bull. Math. Biol.* **56**, 129–146 (1994); K. J. Painter, P. K. Maini and H. G. Othmer, *J. Math. Biol.* **41**, 285 (2000).
- [26] A. J. Ekstrand, C. D. James, W. K. Cavenee, B. Seliger, R. F. Pettersson, and V. P. Collins, *Cancer Res.* **51**, 2164 (1991).
- [27] J. Folkman and M. Hochberg, *J. Exp. Med.* **138**, 745 (1973).
- [28] C. K. N. Li, *Cancer* **50**, 2066 (1982).
- [29] J. P. Freyer, *Cancer Res.* **48**, 2432 (1988).
- [30] J. P. Freyer and R. M. Sutherland, *Cancer Res.* **46**, 3504 (1986).
- [31] H. M. Byrne and M. Chaplain, *Math. Biosci.* **135**, 187 (1996).
- [32] Note that the characteristic time, τ , and length, λ , scales are related to the diffusivity through the relation $\lambda^2/\tau \sim \mu_M \sim \varepsilon^2$. This motivates a change of variable $x \rightarrow x/\varepsilon$.
- [33] J. Xin, *SIAM Rev.* **42**, 161 (2000).
- [34] R. A. Fisher, *Ann. Eugenics* VII 355, (1936); A. Kolmogorov, I. Petrosvky and N. Piscounov, *Moscow Univ. Bull. Math. A* 1, 1 (1937).
- [35] Fisher's equation has a minimal speed v_0 and a continuum of speeds $v > v_0$, which depend on the boundary conditions. In our case we have a finite domain with no flux boundary conditions.
- [36] See A.-L. Barabási and H. E. Stanley, *Fractal Concepts in Surface Growth* (Cambridge University Press, Cambridge, 1995). and references therein.
- [37] J. Müller and W. van Saarloos, *Phys. Rev. E* **65**, 061111 (2002).
- [38] M. R. Chicoine and D. L. Silbergeld, *Neurosurgery* **82**, 615 (1995); R. K. Jain, *Cancer Res.* **47**, 3039 (1987).
- [39] A. H. Nayfeh, *Introduction to Perturbation Techniques* (Wiley, New York, 1981).
- [40] P. C. Fife, *Dynamics of Internal Layers and Diffusive Interfaces*, (SIAM, Philadelphia, PA, 1988).
- [41] R. F. Almgren, *SIAM J. Appl. Math.* **59**, 2086 (1999).
- [42] J. S. Langer, *Rev. Mod. Phys.* **52**, 1 (1980).
- [43] A. Karma and W.-J. Rappel, *Phys. Rev. E* **60**, 3614 (1999).
- [44] P. G. Saffman and G. I. Taylor, *Proc. R. Soc. London, Ser. A* **245**, 312 (1958); D. Bensimon, L. Kadano, S. Liang, B. I. Shraiman, and C. Tang, *Rev. Mod. Phys.* **58**, 977 (1986).
- [45] We have placed the initial flat tumor at a constant value of the x coordinate, that is: $u(x, y, t=0) = \delta(x-x_0)$. This choice and the initial condition for q , Eq. (45) imply that the system of equations only depends on x and is independent of y . We are dealing with an effectively one-dimensional system.
- [46] P. Grindrod, *The Theory and Applications of Reaction-Diffusion Equations: Patterns and Waves* (Oxford University Press, New York, 1996).
- [47] F. Brightman and D. Fell, *FEBS Lett.* **482**, 169 (2000); B. Schoeberl, C. Eichler-Jonsson, E. D. Gilles, and G. Muller, *Nat. Biotechnol.* **20**, 370 (2002).
- [48] S. H. Strogatz, *Nonlinear Dynamics and Chaos: With Applications to Physics, Biology, Chemistry and Engineering* (Perseu, New York, 1994).
- [49] Notice that the numerator of Eq. (56) is positive (the production term $R_C^{(p)}$ is larger than the $R_C^{(d)}$ consumption term) and the denominator R_M is always a positive function of both arguments.
- [50] Notice that the numerator of Eq. (56) is positive but decreases as U increases (the $R_C^{(d)}$ consumption rate catches up with the production term $R_C^{(p)}$).
- [51] J. Valenciano and M. A. J. Chaplain, *Math. Models Meth. Appl. Sci.* **14**, 165 (2004).